

Spiral structure of the Third Galactic Quadrant and the solution to the Canis Major debate

A. Moitinho,^{1*} R. A. Vázquez,² G. Carraro,^{3†} G. Baume,² E. E. Giorgi² and W. Lyra⁴

¹CAAUL, Observatório Astronómico de Lisboa, Tapada da Ajuda, 1349-018 Lisboa, Portugal

²Facultad de Ciencias Astronómicas y Geofísicas de la UNLP, IALP-CONICET, Paseo del Bosque s/n 1900, La Plata, Argentina

³ANDES Fellow, Departamento de Astronomía, Universidad de Chile, Chile, and Astronomy Department, Yale University, USA

⁴Department of Astronomy and Space Physics, Uppsala Astronomical Observatory, Box 515, 751 20 Uppsala, Sweden

Accepted ?. Received ?; in original form ?

ABSTRACT

With the discovery of the Sagittarius dwarf spheroidal (Ibata et al. 1994), a galaxy caught in the process of merging with the Milky Way, the hunt for other such accretion events has become a very active field of astrophysical research. The identification of a stellar ring-like structure in Monoceros, spanning more than 100 degrees (Newberg et al. 2002), and the detection of an overdensity of stars in the direction of the constellation of Canis Major (CMA; Martin et al. 2004), apparently associated to the ring, has led to the widespread belief that a second galaxy being cannibalised by the Milky Way had been found. In this scenario, the overdensity would be the remaining core of the disrupted galaxy and the ring would be the tidal debris left behind. However, unlike the Sagittarius dwarf, which is well below the Galactic plane and whose orbit, and thus tidal tail, is nearly perpendicular to the plane of the Milky Way, the putative CMA galaxy and ring are nearly co-planar with the Galactic disk. This severely complicates the interpretation of observations. In this letter, we show that our new description of the Milky Way leads to a completely different picture. We argue that the Norma-Cygnus spiral arm defines a distant stellar ring crossing Monoceros and the overdensity is simply a projection effect of looking along the nearby local arm. Our perspective sheds new light on a very poorly known region, the third Galactic quadrant (3GQ), where CMA is located.

Key words: Galaxy: structure — open clusters and associations: general — Galaxy: stellar content — galaxies: dwarf

1 INTRODUCTION

The announced detection of a galaxy in CMA (Martin et al. 2004) centred at Galactic coordinates $l = 240^\circ$, $b = -8^\circ$ and at a distance of around 8 kpc from the Sun (Martin et al. 2004; Martínez-Delgado et al. 2005), has produced considerable excitement reaching well beyond the astrophysical community. Independently of how fascinating the idea, the CMA galaxy scenario can be used to address several important astrophysical questions: it is the closest galaxy detected so far, it can be used for a detailed study of the merging process. In having an orbit that is nearly co-planar with the Galactic disc, it can contribute to build up the thick disc thus favouring models of galaxy accretion as the origin of this

still poorly understood component. Finally, it would bring the number of observed nearby low mass satellites of the Milky Way closer to that expected from cosmological simulations (Klypin et al. 1999) of galaxy assembly.

If the presence of a galaxy so close to the Sun offers these unique opportunities, it also requires a detailed knowledge of the structure of the Milky Way to disentangle and understand the complex interplay between both systems. Unfortunately, little attention has been paid to the 3GQ in the past and apart from the presence of the Galactic warp, little is known about its structure. In particular, spiral structure has not been clearly mapped (Rusell 2003).

Apart from the ring and the overdensity, deep colour-magnitude diagrams (CMDs) have been considered to provide additional evidence supporting the reality of the CMA galaxy. By comparing CMDs with stellar evolution models, studies have found the CMA galaxy to be at distance of 8 kpc and to have an age of 4–10 Gyr (Bellazzini et al. 2004;

* E-mail: andre@oal.ul.pt (AM)

† on leave from Dipartimento di Astronomia, Università di Padova, Italy.

Martínez-Delgado et al. 2005). Although the CMDs do not exhibit clear post main-sequence signatures expected for a 4-10 Gyr population (Martínez-Delgado et al. 2005) (red clump or red giant branch, horizontal branch, RR-Lyrae), a distinctive feature, popularised as the Blue Plume (BP; see Fig. 1) has been taken as strong evidence for the existence of the CMa galaxy (Bellazzini et al. 2004; Dinescu et al. 2005; Martínez-Delgado et al. 2005). The BP has been modelled and interpreted as the last burst of star formation in that galaxy 1-2 Gyr ago (which, given that it is a 1-2 Gyr population, should also have a red clump). This piece of evidence has been taken to be an unambiguous indicator of the reality of CMa given that it does not correspond to any known Galactic component. Additionally, the narrowness of the BP, which is indicative of a small distance spread, has been taken as evidence for a compact, possibly bound system (Martínez-Delgado et al. 2005). The absence of a clear post main-sequence is ascribed to heavy contamination by the Galactic field population.

We have recently found (Carraro et al. 2005) that the BP is actually composed of a young population less than 100 Myr old. Except for the cluster sequence which is well detached from the rest of the stars, the CMD of the field around the open cluster NGC 2362 shown in Fig. 1 is identical to the one obtained in another study (Martínez-Delgado et al. 2005) at $l=240^\circ$, $b=-8^\circ$, not far from NGC 2362, and used as proof for the existence of the CMa galaxy. In particular, the BPs have the same position, shape and extension, but we find the BP in Fig. 1 to be much younger and farther away, at 10.8 kpc.

The enormous discrepancy between our study and the others deserves a closer look. The photometric analysis presented in other studies were exclusively limited to CMDs. It is well known that the determination of fundamental parameters - reddening, distance, age and metallicity - is affected by a number of degeneracies (that are readily admitted by the authors) when using a single CMD: different sets of solutions are equally acceptable within observational errors. Those studies have relied on complex modelling of the observed CMDs including the expected Galactic field in that direction. Trial and error changes to the galaxy's fundamental parameters, number of stars and star formation history are made until the synthetic and observed diagrams are considered to match. But even given the rigour of the modelling, the degeneracies persist. Furthermore, the descriptions of the expected Galactic field are also synthetic. Because in these models the contributions from the halo, thick and thin discs do not reproduce the BP, it has been argued that the BP does not correspond to any known Galactic component. These models do not include spiral arms in the region of the 3GQ under analysis.

Our results are based on UBVR_I five band photometry which *does* allow the determination of unique solutions. The reason is that, apart from CMDs, two-colour diagrams (TCDs), which are distance independent, are also used in the analysis. Moreover, when TCDs are built using U band data (not used in the other studies), reddening and spectral types of early type stars can be uniquely derived. Furthermore, metallicity does not affect the colours of these stars significantly. Hence the only unknowns that remain in the CMD analysis are distance and age, which can also be uniquely derived provided that the photometry is deep

enough so that a population sequence appears with a well defined morphology. Briefly, multi-band photometry including U measurements provides direct determinations of reddening and spectral type whereas single CMD analysis does not.

Young open clusters have long been recognised as privileged spiral tracers (Becker & Fenkart 1970). Their distances can be better determined than those of individual stars and their youth keeps them close to the spiral arms where they were born. Over the last 10 years we have collected observations resulting in a unique data set of stellar photometry in the fields of many open star clusters (Moitinho 2001; Moitinho et al. 2001; Carraro & Baume 2003; Baume et al. 2004; Moitinho et al. 2006). A sample of 61 open clusters has been obtained with the goal of tracing the detailed structure of the Galactic disk in the 3GQ, which we present and discuss in this letter.

2 RESULTS

The clusters' basic parameters (reddening, distance and age) have been derived via Zero Age Main Sequence (ZAMS) and isochrone fits to the cluster sequences in different photometric diagrams. This is a standard and solid method that has been used in open cluster studies for several decades.

From the 61 clusters in our sample, 25 were determined to be younger than 100 million years. These are listed in Table 1 and plotted in Fig. 2 which represents the third quadrant of the Galactic plane seen from above. Also plotted, are the BPs detected in the backgrounds of several clusters. A strip about 1.5 kpc wide, extending from $l=210^\circ$ to $l=260^\circ$, spanning distances between 6 and 11 kpc depending on the line of sight, can be seen at the position expected for the Outer (Norma-Cygnus) arm. This strip is mainly composed of BP detections, but also contains a few clusters. On the X-Z projection, the putative outer arm members remain close to the formal Galactic plane ($b=0^\circ$) up to $l=220^\circ$ where the spiral arm starts descending, reaching around 1 kpc below the plane at $l=240-250^\circ$. The bending of the arm is a clear signature of the Galactic stellar warp. This new optical detection of the Norma-Cygnus arm, extending from $l=210^\circ$ to $l=260^\circ$, confirms our previous interpretation of the BP as a spiral tracer and our optical detection of the outer arm based on fewer points (Carraro et al. 2005). That the BP appears so tight in the CMDs is then a natural consequence of the arm's limited depth along each line of sight and is not, in this case, a signature of a compact and possibly bound system as previously used as an argument in favour of the CMa galaxy (Martínez-Delgado et al. 2005). The youth of the BP also explains why no 1-2 Gyr red clump is evident at 8 kpc. Fig. 2 also reveals the presence of a few other BPs. These would also be considered a non-Galactic population, but in this case they are much closer than the proposed distance to the CMa galaxy.

We now focus on the stellar groups marked with a lighter tone. These groups are distributed between $l=190^\circ$ and $l=270^\circ$, but seem to form an elongated structure between $l=230^\circ$ and $l=250^\circ$ stretching toward the outer Galaxy. We interpret this structure as the probable extension of the local (Orion) arm in the third quadrant. It appears that the Orion arm stretches outward reaching and

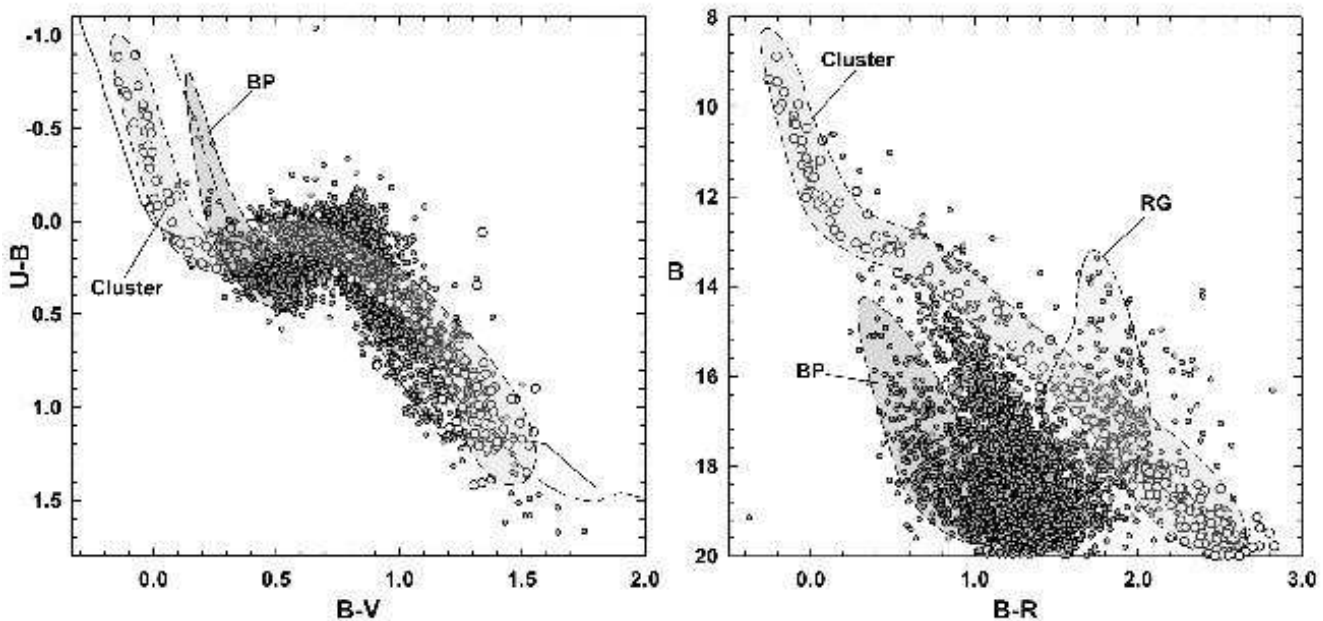


Figure 1. Two-colour (TCD; left) and colour-magnitude (CMD; right) diagrams of a 9×9 field around the open star cluster NGC 2362 ($l=238.18^\circ, b=-5.55^\circ$). Shaded areas roughly separate the regions occupied by three stellar components: members of the cluster NGC 2362 -also shown with large open circles; the blue plume stars, BP, and the red giant stars, RG. The RG region is not shaded on the TCD to avoid confusion. Small grey filled circles indicate the galactic field dwarf population. For guidance, we have superposed on the TCD the intrinsic locus -continuous curve- for dwarf stars (Schmidt-Kaler 1982) and the same curve shifted to account for the effect of reddening -dashed curve- to fit the average BP stars. It can be seen on the TCD that the BP includes stars with spectral types B5-A5, meaning unambiguously that it is a young population less than 100 Myr old. Unlike the CMD where BP stars, cluster members and the field population are well detached, the TCD is entangled for cluster members and BP stars of late B- and early A-types. In the CMD, no obvious overdensity is seen in the RG zone (expected position for the red clump of a 4-10 Gyr galaxy at a distance of 8 kpc).

crossing the Perseus arm. Despite the small number of objects, a few clusters at $l \approx 245^\circ$, and one at $l \approx 185^\circ$, appear to be tracing Perseus, although less evidently at the intersection with the local arm.

To further assess this tentative picture, we have plotted the distribution of CO molecular clouds (kindly provided by J. May and L. Bronfman ahead of publication and also from their previous survey; May et al. 1997). Only clouds more massive than $0.5 \times 10^5 M_\odot$ are shown. The remarkable coincidence of stars and clouds in the outer arm, already stressed by us (Carraro et al. 2005), lends further support to the interpretation of this structure as being a spiral arm and not a tidal tail composed of an old population. The distribution of clouds shows how between $l=180^\circ$ and $l=210^\circ$ the arm becomes very distant from the Sun, which is likely the reason why very distant young clusters have not been optically identified. A good correspondence between the stellar positions and the CO clouds is again found for the region between the Sun and the outer arm (only data from the older survey is available here), although not as good as the one found with the newer CO data in the outer arm. In particular, the Perseus arm is traced by concentrations of CO clouds around $l \approx 220, 235$ and 260° . The lower panel shows that the gas also follows the vertical trend found for the stars in the outer arm. It is interesting to note that a picture in some aspects not very different from the one we have just established has been suggested more than 25 years ago

(Moffat et al. 1979). In particular, that the local arm starts tangent to the Carina-Sagittarius arm in the first quadrant at $l \approx 60^\circ$, and then probably crosses the Perseus arm at $l \approx 240^\circ$, although not as clearly as in this work (likely due to the limited depth of the older photoelectric photometry).

With these results in mind, we can address the CMA overdensity. Although there is no consensus about the exact centre of the overdensity, it is generally accepted that it is around $l = 240^\circ, b = -7^\circ$. From Fig. 2 it is readily seen, both in the gas and in the clusters, that this is the approximate direction of the proposed extension of the Orion arm into the 3GQ. It is therefore quite probable that we should find an overdensity of stars along this line of sight. Indeed, looking along the local arm right through the middle leads us to predict $l \approx 245^\circ$ as the maximum density longitude. Interestingly, the latest estimate of the centre using red clump stars (Bellazzini et al. 2006) is similarly at $l \approx 245^\circ$. It is also worth noticing that the angle comprised by most of the local arm extension roughly corresponds to the area claimed to contain the overdensity. We further notice that this area should be neither much smaller, due to the presence of the local arm, nor much larger, due to the presence of the CO cloud complexes around $l \approx 245^\circ$ and 260° which will limit visibility and introduce a border effect on the observed overdensity. In this context, we find that the CMA overdensity is not the core of a galaxy, but simply the result of looking along the extension of the local arm in the third quadrant.

Table 1. Parameters for clusters and blue plumes. l,b are Galactic longitude and latitude; Dist is the the heliocentric distance; X,Y,Z are Galactic Cartesian coordinates; RGC is the distance to the centre of the Galaxy adopting 8.5 Kpc for the Solar Galactocentric distance.

Field	l ($^{\circ}$)	b ($^{\circ}$)	Dist (kpc)	Age (Myr)	X (kpc)	Y (kpc)	Z (kpc)	RGC (kpc)	Constellation
NGC2129	186.55	+0.06	2.19	10	-0.25	2.18	0.00	10.68	Gemini
S203	210.80	-2.56	8.05	10	-4.12	6.91	-0.36	15.95	Monoceros
Dolidze25	211.20	-1.32	6.33	10	-3.28	5.41	-0.15	14.29	Monoceros
Bochum2	212.30	-0.39	6.31	5	-3.37	5.33	-0.04	14.24	Monoceros
S285	213.80	+0.61	7.70	10	-4.28	6.40	0.08	15.50	Monoceros
BP2232	214.60	-7.41	6.22	<100	-3.50	5.08	-0.80	14.02	Monoceros
NGC2232	214.60	-7.41	0.34	40	-0.19	0.28	-0.04	8.78	Monoceros
S289	218.80	-4.55	9.46	10	-5.91	7.35	-0.75	16.93	Monoceros
NGC2302	219.28	-3.10	1.37	40	-0.87	1.06	-0.07	9.60	Monoceros
NGC2302	219.38	-3.10	7.48	90	-4.74	5.77	-0.40	15.04	Monoceros
NGC2335	223.62	-1.26	1.79	79	-1.23	1.30	-0.04	9.87	Canis Major
NGC2353	224.66	+0.42	1.23	79	-0.86	0.87	0.01	9.41	Canis Major
BP33	225.40	-3.12	7.69	<100	-5.47	5.39	-0.42	14.93	Canis Major
BP7	225.44	-4.58	9.04	<100	-6.42	6.32	-0.72	16.15	Canis Major
NGC2401	229.67	+1.85	6.31	20	-4.81	4.08	0.20	13.47	Puppis
NGC2414	231.41	+1.94	5.62	16	-4.39	3.50	0.19	12.78	Puppis
BP1	232.33	-7.31	7.69	<100	-6.04	4.66	-0.98	14.48	Canis Major
Bochum5	232.56	0.68	2.69	60	-2.14	1.64	0.03	10.36	Puppis
S305	233.80	-0.18	6.11	10	-4.93	3.61	-0.02	13.07	Puppis
S309	234.80	-0.20	7.01	10	-5.73	4.04	-0.02	13.79	Puppis
BP2383	235.27	-2.43	8.79	<100	-7.22	5.00	-0.37	15.31	Canis Major
NGC2384	235.39	-2.42	2.88	13	-2.37	1.63	-0.12	10.41	Canis Major
BP2384	235.39	-2.42	8.79	<100	-7.23	4.99	-0.37	15.30	Canis Major
BP2432	235.48	+1.78	6.00	<100	-4.94	3.40	0.19	12.88	Puppis
NGC2367	235.63	-3.85	2.03	5	-1.67	1.14	-0.14	9.79	Canis Major
BP2367	235.64	-3.85	8.51	<100	-7.01	4.79	-0.57	15.03	Canis Major
NGC2362	238.18	-5.55	1.58	12	-1.34	0.83	-0.15	9.42	Canis Major
BP2362	238.18	-5.55	10.81	<100	-9.14	5.67	-1.05	16.87	Canis Major
Trumpler7	238.21	-3.34	2.04	50	-1.73	1.07	-0.12	9.73	Puppis
BP18	239.94	-4.92	7.87	<100	-6.79	3.93	-0.67	14.16	Canis Major
Ruprecht32	241.50	-0.60	9.68	10	-8.51	4.62	-0.10	15.64	Puppis
Haffner16	242.09	+0.47	3.63	50	-3.21	1.70	0.03	10.69	Puppis
Haffner19	243.04	0.52	5.25	4	-4.68	2.38	0.05	11.84	Puppis
Haffner18	243.11	0.42	7.94	4	-7.08	3.59	0.06	14.01	Puppis
NGC2453	243.35	-0.93	5.25	40	-4.69	2.35	-0.09	11.83	Puppis
NGC2439	246.41	-4.43	4.57	10	-4.18	1.82	-0.35	11.14	Puppis
BP2439	246.41	-4.43	10.91	<100	-9.97	4.35	-0.84	16.27	Puppis
Ruprecht35	246.63	-3.24	5.32	70	-4.88	2.11	-0.30	11.67	Puppis
BP2533	247.81	+1.29	6.49	<100	-6.01	2.45	0.15	12.49	Puppis
Ruprecht47	248.25	-0.19	4.37	70	-4.06	1.62	-0.01	10.90	Puppis
NGC2571	249.10	+3.54	1.38	50	-1.29	0.49	0.09	9.08	Puppis
Ruprecht48	249.12	-0.59	6.03	70	-5.63	2.15	-0.06	12.05	Puppis
Ruprecht55	250.68	+0.76	4.59	10	-4.33	1.52	0.06	10.91	Puppis
BP55	250.68	+0.76	6.98	<100	-6.59	2.31	0.09	12.66	Puppis
BP2477	253.56	-5.84	11.69	<100	-11.15	3.29	-1.19	16.23	Puppis
NGC2547	264.45	-8.53	0.49	63	-0.48	0.05	-0.07	8.56	Vela
Pismis8	265.09	-2.59	2.00	7	-1.99	0.17	-0.09	8.90	Vela
NGC2910	275.29	-1.17	1.32	70	-1.31	-0.12	-0.03	8.48	Vela

A previous alternative explanation for the overdensity has been proposed in which the overdensity is a signature of the Galactic warp (Momany et al. 2004), although it does not fully explain the Monoceros ring. This has induced a lively debate where the warp explanation has been partially rebated (Martin et al. 2004). But that counter attack, although favouring the CMa galaxy, also pointed out that its kinematics was compatible with the velocities of a distant arm detected in the fourth quadrant (McClure-Griffiths et al. 2004). Since this distant arm is

quite likely the continuation of the Norma arm according to model predictions (Cordes & Lazio 2002), the kinematic result then further supports our picture.

Given the evidence we have presented here, our scenario is the only one that presently accounts for, and explains, all the observational results. As a final remark, we note that no ad-hoc new spiral arms had to be introduced. All the spiral features we evoke are simply previously unclear extensions of well known arms whose existence has been repeatedly established during the last few decades. In this context, the

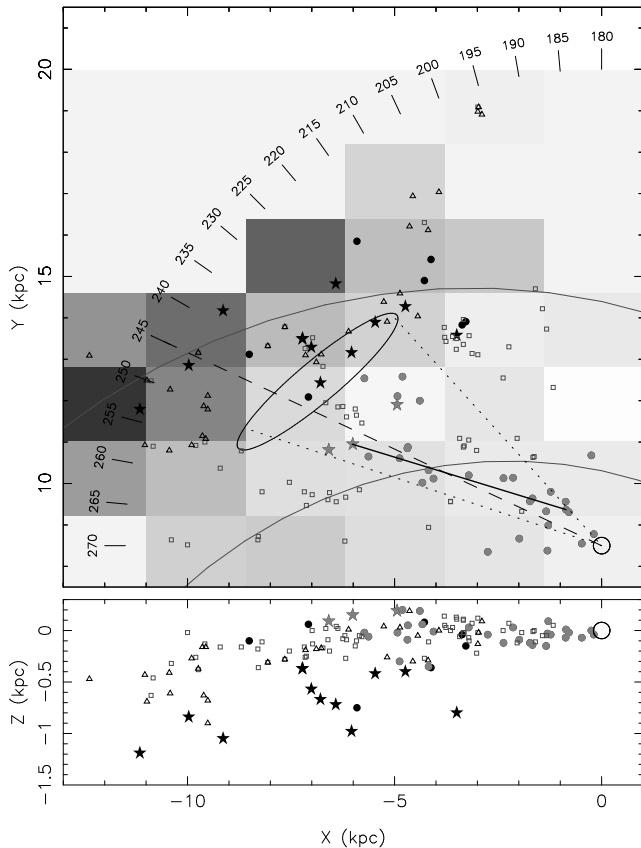


Figure 2. Distribution of young star clusters, BPs and massive CO clouds in the third quadrant of the Milky Way. Clusters are depicted as filled circles, BPs as stars. Darker symbols indicate the populations associated to the Norma-Cygnus (Outer) arm. CO clouds are plotted as empty triangles (newer data) and squares (older data). The coordinate system is right handed with its origin at the Galactic centre. Y indicates the direction of the Sun, Z points toward the north Galactic pole and X grows in the direction of Galactic rotation at the position of the Sun. The Sun is marked as a larger circle at $X=0$, $Y=8.5$, $Z=0$ kpc. The upper panel provides a view of the Galactic disc as seen from above. A longitude scale is also provided. The grid of grey squares illustrates the height of the disc with respect to the formal Galactic plane ($b = 0^\circ$): lighter tones are closer to the plane and darker tones are deeper below. The tone scale is linear and each tone corresponds to the average Z in the cell. A clear picture of the Galactic warp is easily seen. The two curves that cross the panel are model (Vallée 2005) extrapolations of the Outer and Perseus arms and the solid straight line sketches the local arm. The position and extent of the Canis Major overdensity are indicated by a large ellipse. The dashed line is the line of sight mostly dominated by the local arm and the dotted lines mark the range where the contribution of the local arm appears to be significant. Lower panel: X-Z projection. The signature of the warp is again prominent. It is also readily visible how the the molecular clouds closely follow the stellar distribution.

presence of spiral arms in a region of a spiral galaxy where they are supposed to be, but have not been detected before, is a more natural explanation of the CMA phenomena than a cannibalised galaxy in a nearly co-planar orbit, how exciting it might be.

ACKNOWLEDGMENTS

We thank J. May and L. Bronfman for helpful discussions and for providing results ahead of publication and P.G. Ferreira for language editing. A.M. acknowledges grant SFRH/BPD/19105/2004 from *FCT* (Portugal). G.C. acknowledges *Fundación Andes*. R.A.V., G.C., G.B. and E.G. acknowledge *Programa Científico-Tecnológico Argentino-Italiano SECYT-MAE IT/PA03-U11/077-2004-2005*. This study made use of Simbad and WEBDA databases.

REFERENCES

- Baume G., Moitinho A., Giorgi E. E., Carraro G., Vázquez R. A., 2004, *A&A*, 417, 961
- Becker W., Fenkart R. B., 1970, in *IAU Symp. 38: The Spiral Structure of our Galaxy Vol. 38, Galactic Clusters and H II Regions*. p. 205
- Bellazzini M., Ibata R., Martin N., Lewis G. F., Conn B., Irwin M. J., 2006, *MNRAS*, 366, 865
- Bellazzini M., Ibata R., Monaco L., Martin N., Irwin M. J., Lewis G. F., 2004, *MNRAS*, 354, 1263
- Carraro G., Baume G., 2003, *MNRAS*, 346, 18
- Carraro G., Vázquez R. A., Moitinho A., Baume G., 2005, *ApJ*, 630, L153
- Cordes J. M., Lazio T. J. W., 2002, *astro-ph/0207156*
- Dinescu D. I., Martínez-Delgado D., Girard T. M., Peñarrubia J., Rix H.-W., Butler D., van Altena W. F., 2005, *ApJ*, 631, L49
- Ibata R. A., Gilmore G., Irwin M. J., 1994, *Nat*, 370, 194
- Klypin A., Kravtsov A. V., Valenzuela O., Prada F., 1999, *ApJ*, 522, 82
- Martin N. F., Ibata R. A., Bellazzini M., Irwin M. J., Lewis G. F., Dehnen W., 2004, *MNRAS*, 348, 12
- Martin N. F., Ibata R. A., Conn B. C., Lewis G. F., Bellazzini M., Irwin M. J., McConnachie A. W., 2004, *MNRAS*, 355, L33
- Martínez-Delgado D., Butler D. J., Rix H.-W., Franco Y. I., Peñarrubia J., Alfaro E. J., Dinescu D. I., 2005, *ApJ*, 633, 205
- May J., Alvarez H., Bronfman L., 1997, *A&A*, 327, 325
- McClure-Griffiths N. M., Dickey J. M., Gaensler B. M., Green A. J., 2004, *ApJ*, 607, L127
- Moffat A. F. J., Jackson P. D., Fitzgerald M. P., 1979, *A&AS*, 38, 197
- Moitinho A., 2001, *A&A*, 370, 436
- Moitinho A., Alves J., Huéramo N., Lada C. J., 2001, *ApJ*, 563, L73
- Moitinho A., Carraro G., Baume G., Vázquez R. A., 2006, *A&A*, 445, 493
- Momany Y., Zaggia S. R., Bonifacio P., Piotto G., De Angelis F., Bedin L. R., Carraro G., 2004, *A&A*, 421, L29
- Newberg H. J., Yanny B., Rockosi C., Grebel E. K., Rix H.-W., Brinkmann J., Csabai I., Hennessy G., Hindsley R. B., Ibata R., Ivezić Z., Lamb D., Nash E. T., Odenkirchen M., Rave H. A., Schneider D. P., Smith J. A., Stolte A., York D. G., 2002, *ApJ*, 569, 245
- Russeil D., 2003, *A&A*, 397, 133
- Schmidt-Kaler T., 1982, *Landolt-Börnstein, Group VI, Vol. 2b, Stars and Star Clusters*. Springer, Berlin, p. 15
- Vallée J. P., 2005, *AJ*, 130, 569